Measurement of the Generalized Forward Spin Polarizabilities of the Neutron

M. Amarian,[24] L. Auerbach,[20] T. Averett,[6,23] J. Berthot,[4] P. Bertin,[4] W. Bertozzi,[11] T. Black,[11] E. Brash,[16] D. Brown,[10] E. Burtin,[18] J. Calarco,[13] G. Cates,[15,22] Z. Chai,[11] J.-P. Chen,[6] Seonho Choi,[20] E. Chudakov,[6] E. Cisbani,[5] C.W. de Jager,[6] A. Deur,[4,6,22] R. DiSalvo,[4] S. Dieterich,[17] P. Djawotho,[23] J. M. Finn,[23] K. Fissum,[11] H. Fonvieille,[4] S. Frullani,[5] H. Gao,[11] J. Gao,[1] F. Garibaldi,[5] A. Gasparian,[3] S. Gilad,[11] R. Gilman,[6,17] A. Glamazdin,[9] C. Glashausser,[17] E. Goldberg,[1] J. Gomez,[6] V. Gorbenko,[9] J.-O. Hansen,[6] B. Hersman,[13] R. Holmes,[19] G. M. Huber,[16] E. Hughes,[1] B. Humensky,[15] S. Incerti,[20] M. Iodice,[5] S. Jensen,[1] X. Jiang,[17] C. Jones,[1] G. Jones,[8] M. Jones,[23] C. Jutier,[4,14] A. Ketikyan,[24] I. Kominis,[15] W. Korsch,[8] K. Kramer,[23] K. Kumar,[12,15] G. Kumbartzki,[17] M. Kuss,[6] E. Lakuriqi,[20] G. Laveissiere,[4] J. Lerose,[6] M. Liang,[6] N. Liyanage,[6,11] G. Lolos,[16] S. Malov,[17] J. Marroncle,[18] K. McCormick,[14] R. Mckeown,[1] Z.-E. Meziani,[20] R. Michaels,[6] J. Mitchell,[6] Z. Papandreou,[16] T. Pavlin,[1] G. G. Petratos,[7] D. Pripstein,[1] D. Prout,[7] R. Ransome,[17] Y. Roblin,[4] D. Rowntree,[11] M. Rvachev,[11] F. Sabatie,[14] A. Saha,[6] K. Slifer,[20] P. Souder,[19] T. Saito,[21] S. Strauch,[17] R. Suleiman,[7] K. Takahashi,[21] S. Teijiro,[21] L. Todor,[14] H. Tsubota,[21] H. Ueno,[21] G. Urciuoli,[5] R. Van der Meer,[6,16] P. Vernin,[18] H. Voskanian,[24] B. Wojtsekhowski,[6] F. Xiong,[11] W. Xu,[11] J.-C Yang,[2] B. Zhang,[11] and P. A. Żołnierczuk[8]

(Jefferson Lab E94010 Collaboration)

[1]*California Institute of Technology, Pasadena, California 91125 USA*
[2]*Chungnam National University, Taejon 305-764, Korea*
[3]*Hampton University, Hampton, Virginia 23668 USA*
[4]*LPC IN2P3/CNRS, Université Blaise Pascal, F-63170 Aubière Cedex, France*
[5]*Istituto Nazionale di Fiscica Nucleare, Sezione Sanità, 00161 Roma, Italy*
[6]*Thomas Jefferson National Accelerator Facility, Newport News, Virginia 23606 USA*
[7]*Kent State University, Kent, Ohio 44242 USA*
[8]*University of Kentucky, Lexington, Kentucky 40506 USA*
[9]*Kharkov Institute of Physics and Technology, Kharkov 310108, Ukraine*
[10]*University of Maryland, College Park, Maryland 20742 USA*
[11]*Massachusetts Institute of Technology, Cambridge, Massachusetts 02139 USA*
[12]*University of Massachusetts-Amherst, Amherst, Massachusetts 01003 USA*
[13]*University of New Hampshire, Durham, New Hampshire 03824 USA*
[14]*Old Dominion University, Norfolk, Virginia 23529 USA*
[15]*Princeton University, Princeton, New Jersey 08544 USA*
[16]*University of Regina, Regina, SK S4S 0A2, Canada*
[17]*Rutgers, The State University of New Jersey, Piscataway, New Jersey 08855 USA*
[18]*CEA Saclay, DAPNIA/SPHN, F-91191 Gif/Yvette, France*
[19]*Syracuse University, Syracuse, New York 13244 USA*
[20]*Temple University, Philadelphia, Pennsylvania 19122 USA*
[21]*Tohoku University, Sendai 980, Japan*
[22]*University of Virginia, Charlottesville, Virginia 22904 USA*
[23]*The College of William and Mary, Williamsburg, Virginia 23187 USA*
[24]*Yerevan Physics Institute, Yerevan 375036, Armenia*

(Received 2 June 2004; published 5 October 2004)

The generalized forward spin polarizabilities γ_0 and δ_{LT} of the neutron have been extracted for the first time in a Q^2 range from 0.1 to 0.9 GeV^2. Since γ_0 is sensitive to nucleon resonances and δ_{LT} is insensitive to the Δ resonance, it is expected that the pair of forward spin polarizabilities should provide benchmark tests of the current understanding of the chiral dynamics of QCD. The new results on δ_{LT} show significant disagreement with chiral perturbation theory calculations, while the data for γ_0 at low Q^2 are in good agreement with a next-to-leading-order relativistic baryon chiral perturbation theory calculation. The data show good agreement with the phenomenological MAID model.

DOI: 10.1103/PhysRevLett.93.152301 PACS numbers: 14.20.Dh, 11.55.Hx, 12.38.Qk, 25.30.–c

The study of nucleon structure is one of the most important subjects of modern physics. The dominant interaction responsible for nucleon structure is the strong interaction. High energy experiments have established quantum chromodynamics (QCD) as the gauge theory describing the strong interaction between quarks and gluons, which are the elementary constituents of the nucleon. At high energies, observables in QCD can be

calculated perturbatively since the running coupling constant is small. However, at low energies, the coupling constant becomes increasingly large and quarks and gluons are confined to color singlet objects known as hadrons. There, nucleon structure is usually described in terms of hadronic degrees of freedom, namely, baryons and mesons. Chiral perturbation theory (χPT) is applicable in this region. The intermediate energy region is described by phenomenological models and will eventually be described by lattice QCD calculations.

The polarizabilities of the nucleon are fundamental observables that characterize nucleon structure. They are related to integrals of the nucleon excitation spectrum. The electric and magnetic polarizabilities measure the nucleon's response to an external electromagnetic field. Because the polarizabilities can be linked to the forward Compton scattering amplitudes, real photon Compton scattering experiments [1] were performed to measure these polarizabilities. Another polarizability, associated with a spin-flip, is the forward spin polarizability γ_0. It has been measured in an experiment at Mainz accelerator [2] with a circularly polarized photon beam on a longitudinally polarized proton target. The extension of these quantities to the case of virtual photon Compton scattering with the finite four-momentum-squared Q^2 leads to the concept of the generalized polarizabilities [3]. Generalized polarizabilities are related to the forward virtual Compton scattering amplitudes and the forward doubly virtual Compton scattering (VVCS) amplitudes [4]. With this additional dependence on Q^2, the generalized polarizabilities provide a powerful tool to probe the nucleon structure covering the whole range from the partonic to the hadronic region. In particular, the generalized polarizabilities provide one of the most extensive tests of χPT calculations in the low Q^2 region [4,5]. However, up to now, other than the real photon measurement of γ_0 for the proton from Mainz accelerator, there have been no experimental data available for the generalized spin polarizabilities for either the proton or the neutron.

In this Letter, we present the first results for the neutron generalized forward spin polarizabilities $\gamma_0(Q^2)$ and $\delta_{LT}(Q^2)$ over the Q^2 range from 0.1 to 0.9 $(\mathrm{GeV})^2$. These results were extracted from a measurement of σ_{TT} and σ_{LT}, the doubly polarized transverse-transverse and longitudinal-transverse interference cross sections, or equivalently g_1 and g_2, the two inclusive spin structure functions, in the resonance region. Thomas Jefferson National Accelerator Facility's high intensity polarized electron beam and a high density polarized ^{3}He target were used for the measurement. The polarized ^{3}He target provided an effective polarized neutron target because the ground state of ^{3}He is dominated by the s state, in which the spins of the two protons antialign and cancel. Therefore the spin of the ^{3}He nucleus comes largely from the neutron. Doubly polarized inclusive cross sections were measured at six incident beam energies from 0.86 to 5.1 GeV, all at a fixed scattering angle of 15.5°. Data were collected for both longitudinal and transverse target polarization orientations, enabling the extractions of both σ_{TT} and σ_{LT}. The integrals of σ_{TT} and σ_{LT} of the neutron were extracted from those of ^{3}He following the prescription suggested by Ciofi degli Atti and Scopetta in Ref. [6] to take into account the nuclear corrections. Details of the experiment can be found in Refs. [7] and [8].

Following Ref. [4], an unsubtracted dispersion relation for the spin-flip VVCS amplitude g_{TT} with an appropriate convergence behavior at high energy leads to

$$\mathrm{Re}\tilde{g}_{TT}(\nu, Q^2) = \left(\frac{\nu}{2\pi^2}\right)\mathcal{P}\int_{\nu_0}^{\infty}\frac{K(\nu', Q^2)\sigma_{TT}(\nu', Q^2)}{\nu'^2 - \nu^2}d\nu', \tag{1}$$

where $\tilde{g}_{TT} \equiv g_{TT} - g_{TT}^{\mathrm{pole}}$, g_{TT}^{pole} is the nucleon pole contribution, ν is the energy of the virtual photon, and K is the virtual photon flux factor. The lower limit of the integration ν_0 is the π production threshold on the neutron. A low energy expansion gives

$$\mathrm{Re}\tilde{g}_{TT}(\nu, Q^2) = \left(\frac{2\alpha}{M^2}\right)I_A(Q^2)\nu + \gamma_0(Q^2)\nu^3 + O(\nu^5), \tag{2}$$

with α the electromagnetic fine-structure constant and M the neutron mass. $I_A(Q^2)$ is the coefficient of the $O(\nu)$ term of the Compton amplitude. Equation (2) defines the generalized forward spin polarizability $\gamma_0(Q^2)$. Combining Eqs. (1) and (2), the $O(\nu)$ term yields a sum rule for the generalized Gerasimov-Drell-Hearn (GDH) integral [9–11]: the integration of σ_{TT}, with $1/\nu$ weighting, is proportional to I_A, the coefficient of the $O(\nu)$ term of the VVCS amplitude. From the $O(\nu^3)$ term, one obtains a sum rule for the generalized forward spin polarizability [4]:

$$\begin{aligned}\gamma_0(Q^2) &= \left(\frac{1}{2\pi^2}\right)\int_{\nu_0}^{\infty}\frac{K(\nu, Q^2)}{\nu}\frac{\sigma_{TT}(\nu, Q^2)}{\nu^3}d\nu \\ &= \frac{16\alpha M^2}{Q^6}\int_0^{x_0} x^2\left[g_1(x, Q^2) - \frac{4M^2}{Q^2}x^2 g_2(x, Q^2)\right]dx,\end{aligned} \tag{3}$$

where $x = Q^2/(2M\nu)$ is the Bjorken scaling variable.

Considering the longitudinal-transverse interference amplitude g_{LT}, with the same assumptions, one obtains

$$\mathrm{Re}\tilde{g}_{LT}(\nu, Q^2) = \left(\frac{2\alpha}{M^2}\right)QI_3(Q^2) + Q\delta_{LT}(Q^2)\nu^2 + O(\nu^4), \tag{4}$$

where the $O(1)$ term leads to a sum rule for $I_3(Q^2)$, which relates it to the σ_{LT} integral over the excitation spectrum. The $O(\nu^2)$ term leads to the generalized longitudinal-transverse polarizability [4]:

$$\begin{aligned}\delta_{LT}(Q^2) &= \left(\frac{1}{2\pi^2}\right)\int_{\nu_0}^{\infty}\frac{K(\nu, Q^2)}{\nu}\frac{\sigma_{LT}(\nu, Q^2)}{Q\nu^2}d\nu \\ &= \frac{16\alpha M^2}{Q^6}\int_0^{x_0} x^2[g_1(x, Q^2) + g_2(x, Q^2)]dx.\end{aligned} \tag{5}$$

The basic assumptions leading to the dispersion relations between the forward Compton amplitudes and the generalized spin polarizabilities are the same as those leading to the generalized GDH sum rule. However, since the generalized polarizabilities have an extra $1/\nu^2$ weighting compared to the GDH sum or I_3, these integrals converge much faster, which minimizes the issue of extrapolation to the unmeasured region at large ν. For the kinematics of this experiment, the contributions to the generalized polarizabilities from the unmeasured region are negligible.

At low Q^2, the generalized polarizabilities have been evaluated with χPT calculations [12,13]. One issue in the χPT calculations is how to properly include the nucleon resonance contributions, especially the Δ resonance, which is usually dominating. As was pointed out in Refs. [12] and [13], while γ_0 is sensitive to resonances, δ_{LT} is insensitive to the Δ resonance. Measurements of the generalized spin polarizabilities will be an important step in understanding the dynamics of QCD in the chiral perturbation region.

We will first focus on the low Q^2 region where the comparison with χPT calculations is meaningful and then show the complete data set from Q^2 of 0.1 to 0.9 GeV^2.

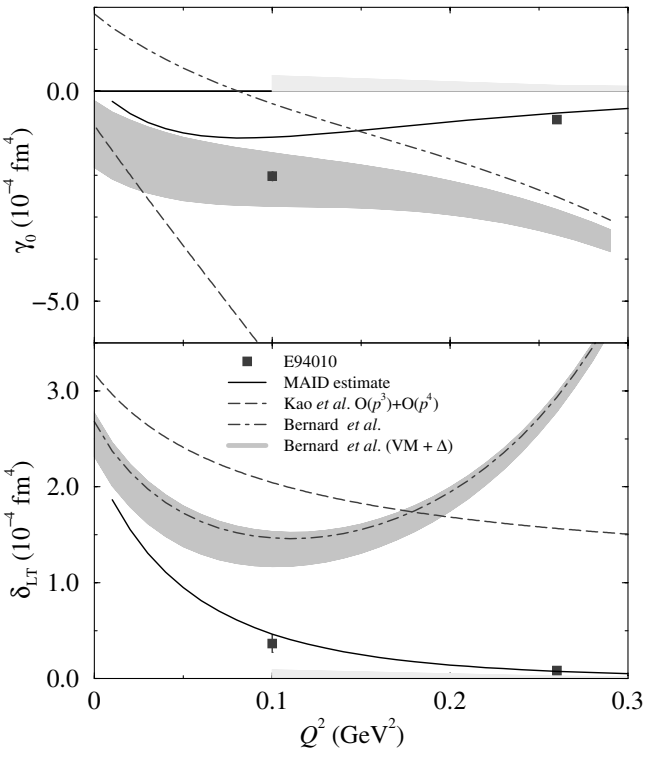

FIG. 1. Forward spin polarizabilities γ_0 (top panel) and δ_{LT} (bottom panel). Solid squares are the results with statistical uncertainties. The light bands are the systematic uncertainties. The dashed curves are the heavy baryon χPT calculation from Ref. [12]. The dot-dashed curves and the dark bands are the relativistic baryon χPT calculation from Ref. [13], without and with the Δ and vector meson contributions, respectively. Solid curves are from the MAID model [14].

The results of $\gamma_0(Q^2)$ for the neutron are shown in the top panel of Fig. 1 as a function of Q^2 for the two lowest Q^2 values of 0.10 and 0.26 GeV^2. The statistical uncertainties are generally smaller than the size of the symbols. The systematic uncertainties are dominated by the uncertainties in the radiative corrections, the spectrometer acceptance, and the beam and target polarization measurements. The data are compared with a next-to-leading-order $O(p^4)$ heavy baryon χPT (HBχPT) calculation [12], a next-to-leading-order relativistic baryon χPT (RBχPT) calculation [13], and the same calculation explicitly including both the Δ resonance and vector meson contributions. Predictions from the MAID model [14] are also shown. At the lowest Q^2 point of 0.1 GeV^2, the RBχPT calculation including the resonance contributions is in good agreement with the experimental result. For the HBχPT calculation without explicit resonance contributions, discrepancies are large even at $Q^2 = 0.1$ GeV^2. This might indicate the significance of the resonance contributions or a problem with the heavy baryon approximation at this Q^2. The higher Q^2 data point is in good agreement with the MAID prediction, but the lowest data point at $Q^2 = 0.1$ GeV^2 is significantly lower, consistent with what was observed for the generalized GDH integral results [7] and the underestimation from MAID for the neutron GDH sum rule at the real photon point [14].

Since the longitudinal-transverse spin polarizability δ_{LT} is insensitive to the dominating Δ resonance contribution, it was believed that δ_{LT} should be more suitable than γ_0 to serve as a testing ground for the chiral dynamics of QCD [12,13]. The bottom panel of Fig. 1 shows δ_{LT} for the neutron compared to χPT calculations and the MAID predictions. It is surprising to see that the data are in significant disagreement with the χPT calculations even at the lowest Q^2, 0.1 GeV^2. This disagreement presents a significant challenge to the present theoretical understanding. The MAID predictions are in good agreement with our results.

Table I lists the experimental results for all Q^2 values. Figure 2 shows the results of both γ_0 and δ_{LT} multiplied by Q^6 along with the MAID and χPT calculations. Also

TABLE I. Results for $\gamma_0(Q^2)$ and $\delta_{LT}(Q^2)$, along with statistical and systematic uncertainties.

Q^2	$\gamma_0 \pm$ stat $\pm$ syst	$\delta_{LT} \pm$ stat $\pm$ syst
(GeV^2)	(10^{-4} fm^4)	(10^{-4} fm^4)
0.10	$-2.02 \pm 0.11 \pm 0.36$	$0.364 \pm 0.092 \pm 0.091$
0.26	$-0.67 \pm 0.015 \pm 0.14$	$0.084 \pm 0.011 \pm 0.025$
0.42	$-0.200 \pm 0.005 \pm 0.039$	$0.018 \pm 0.004 \pm 0.005$
0.58	$-0.084 \pm 0.002 \pm 0.019$	$0.004 \pm 0.002 \pm 0.002$
0.74	$-0.037 \pm 0.001 \pm 0.009$	$0.002 \pm 0.001 \pm 0.001$
0.90	$-0.016 \pm 0.001 \pm 0.004$	$0.001 \pm 0.001 \pm 0.000$

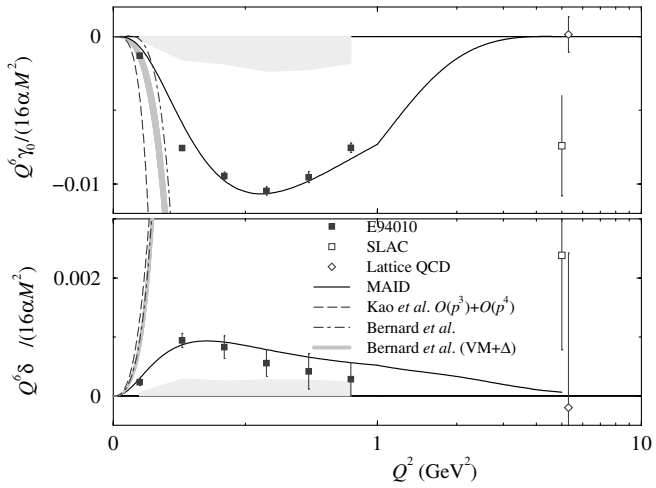

FIG. 2. Forward spin polarizability γ_0 (top panel) and δ_{LT} (bottom panel) with Q^6 weighting. The solid squares are the results with statistical uncertainties. The light bands are the systematic uncertainties. The open squares are the Stanford Linear Accerelator Center data [15], and the open diamonds are the lattice QCD calculations [16]. The curves are the same as in Fig. 1.

shown are the world data [15] and a quenched lattice QCD calculation [16], both at $Q^2 = 5$ GeV^2.

It is expected that, at large Q^2, the Q^6-weighted spin polarizabilities become independent of Q^2 (scaling) [4], and the deep-inelastic-scattering Wandzura-Wilczek relation [17] leads to a relation between γ_0 and δ_{LT}:

$$\delta_{LT}(Q^2) \to \frac{1}{3}\gamma_0(Q^2) \quad \text{as} \quad Q^2 \to \infty. \tag{6}$$

For inclusive deep-inelastic-scattering structure functions and their first moments, the scaling behavior is observed to start around Q^2 of 1 GeV^2, where the higher twist effects become insignificant. For the higher moments the scaling behavior is expected to start at a higher Q^2 than that for the first moments. Our results show that scaling behavior is not observed at $Q^2 < 1$ GeV^2. Again, both results are in good agreement with the MAID model.

In conclusion, we have made the first measurement of the forward spin polarizabilities $\gamma_0(Q^2)$ and $\delta_{LT}(Q^2)$ for the neutron in the Q^2 range from 0.1 to 0.9 GeV^2. The low Q^2 results were compared to next-to-leading-order χPT calculations of two groups. The datum for γ_0 at the lowest Q^2 is in good agreement with the RBχPT calculations including explicit resonance contributions. Although it was expected that χPT calculations should converge faster for δ_{LT} than for γ_0 as a result of smaller resonance contributions, we find significant disagreement between data and both χPT calculations for δ_{LT}. The discrepancy presents a significant challenge to our theoretical understanding at its present level of approximations and might indicate that higher order calculations are needed for $Q^2 \geq 0.1$ GeV^2 and above. Our results, combining with future measurements at even lower Q^2 [18], will provide benchmark tests for our understanding of QCD chiral dynamics. Except at the lowest Q^2 point for γ_0, the rest of the new data agree well with the MAID model. It shows that the current level of phenomenological understanding of the resonance spin structure in these observables is reasonable. In the Q^2 range of this experiment, the expected high-Q^2 scaling behavior has not been observed yet.

We would like to acknowledge the outstanding support of the Jefferson Lab staff. We thank V. Bernard, D. Drechsel, T. Hemmert, B. Holstein, C.W. Kao, Ulf-G. Meissner, L. Tiator, M. Vanderhaeghen, and their collaborators for theoretical support and helpful discussions. This work was supported by the U.S. Department of Energy (DOE), the U.S. National Science Foundation, the European INTAS Foundation, the Italian INFN, and the French CEA, CNRS, and Conseil Régional d'Auvergne. The Southeastern Universities Research Association operates the Thomas Jefferson National Accelerator Facility for the DOE under Contract No. DE-AC05-84ER40150.

[1] V. Olmos de Leon *et al.*, Eur. Phys. J. **A 10**, 207 (2001); J. Tonnison *et al.*, Phys. Rev. Lett. **80**, 4382 (1998).
[2] J. Ahrens *et al.*, Phys. Rev. Lett. **87**, 022003 (2001).
[3] P. A. M. Guichon, G. Q. Liu, and A.W. Thomas, Nucl. Phys. **A 591**, 606 (1995).
[4] D. Drechsel, B. Pasquini, and M. Vanderhaeghen, Phys. Rep. **378**, 99 (2003).
[5] J. Roche *et al.*, Phys. Rev. Lett. **85**, 708 (2000).
[6] C. Ciofi degli Atti and S. Scopetta, Phys. Lett. B **404**, 223 (1997).
[7] M. Amarian *et al.*, Phys. Rev. Lett. **89**, 242301 (2002).
[8] M. Amarian *et al.*, Phys. Rev. Lett. **92**, 022301 (2004).
[9] S. B. Gerasimov, Sov. J. Nucl. Phys. **2**, 598 (1965); S. D. Drell and A. C. Hearn, Phys. Rev. Lett. **16**, 908 (1966).
[10] D. Drechsel, S. S. Kamalov, and L. Tiator, Phys. Rev. D **63**, 114010 (2001).
[11] X. Ji and J. Osborne,J. Phys. G **27**, 127 (2001).
[12] C.W. Kao, T. Spitzenberg, and M. Vanderhaeghen, Phys. Rev. D **67**, 016001 (2003).
[13] V. Bernard, T. R. Hemmert and Ulf-G. Meissner, Phys. Rev. D**67**, 076008 (2003).
[14] D. Drechsel, S. S. Kamalov, and L. Tiator, Phys. Rev. D **63**, 114010 (2001).
[15] P. L. Anthony *et al.*, Phys. Lett. B **493**, 19 (2000); P. L. Anthony *et al.*, Phys. Lett. B **553**, 18 (2003).
[16] M. Gockeler *et al.*, Phys. Rev. D **63**, 074506 (2001).
[17] S. Wandzura and F. Wilczek, Phys. Lett. B **72**, 195 (1977).
[18] J.-P. Chen, A. Deur, and F. Garibaldi, (spokespersons for the Jefferson Lab Experiment No. E97-110), http://hallaweb.jlab.org/experiment/E97-110/.